

JOINT INSTITUTE FOR NUCLEAR RESEARCH
Veksler and Baldin Laboratory of High Energy Physics

FINAL REPORT ON THE SUMMER STUDENT PROGRAM

Study of vorticity and helicity according to model data
from SMASH in Au+Au collisions $\sqrt{s_{NN}} = 11.5$ GeV

Supervisor: Dr. Oleg Valerianovich Teryaev, JINR

Student: Vasily Nikolaev, Russia NRNU MEPHI

Participation Period: August 01 - September 14

Dubna, 2019

1 Abstract

1

2 We study the structure of vorticity and hydrodynamic helicity fields in non-
3 central heavy ion collisions. Using the Simulating Many Accelerated Strongly-
4 interacting Hadrons (SMASH) model we perform the numerical simulations of
5 Au+Au collisions at energy $\sqrt{s_{NN}} = 11.5$ GeV. In this research velocity, vor-
6 ticity and helicity was calculated using different definitions of cell velocity.

7 **Contents**

8	1 Abstract	1
9	2 Introduction	3
10	3 Basic concepts and methodology	4
11	3.1 Velocity and vorticity	4
12	3.2 Helicity	4
13	4 The SMASH model	5
14	4.1 Model overview	5
15	4.2 Event generating	5
16	5 Velocity and vorticity fields	6
17	5.1 Velocity weighting	6
18	5.2 Vorticity calculation	7
19	5.3 Helicity separation	8
20	6 Conclusion	10
21	7 References	11

2 Introduction

23 The high-energy heavy-ion collisions provides us unique opportunity to study
24 strongly interacting matter in laboratory. In peripheral high energy heavy ion
25 collisions the system has a large angular momentum in the direction perpendicular
26 to the reaction plane [1]. After the collision, part of total angular momentum
27 is saved in the quark-gluon plasma. This fraction of the angular momentum is
28 manifested as a shift in the longitudinal momentum density and it has been
29 shown in hydrodynamical computation that this leads to a large shear and vorticity
30 [2]. In hydrodynamics, the vorticity represents the local angular velocity,
31 and it leads to interesting effects. For example may occur phenomena like rotation
32 [3], or even turbulence [4] [5]. Also the large angular momentum may show
33 itself in the polarization of secondary produced particles [6].

3 Basic concepts and methodology

3.1 Velocity and vorticity

We start our studies with the structure of velocity and vorticity fields. We will consider these values as the average for all particles in a given phase volume.

Mathematically the velocity field can be defined as double sum over the particles in phase volume and over all simulated collisions: [7]

$$\vec{v}(x, y, z, t) = \frac{\sum_i \sum_j \vec{P}_{ij}}{\sum_i \sum_j E_{ij}} \quad (1)$$

where \vec{P}_{ij} and $\sum_j E_{ij}$ are the momentum and full energy of particle i in the collision j , respectively.

Another way of calculating velocity field is to sum particle velocities:

$$\vec{v}(x, y, z, t) = \sum_i \sum_j \frac{\vec{P}_{ij}}{E_{ij}} \quad (2)$$

Unlike in classical hydrodynamics, where vorticity is defined as:

$$\omega = \nabla \times \vec{v} \quad (3)$$

several vorticities can be defined in relativistic hydrodynamics according to different physical conditions [6].

3.2 Helicity

Helicity is a pseudoscalar characteristic of vorticity:

$$H = \int dV (\vec{v} * \vec{\omega}) \quad (4)$$

that is associated with a number of interesting phenomena in hydrodynamics and plasma physics, such as turbulent Dynamo and Lagrangian chaos [7]. It is the extent to which corkscrew-like motion occurs

55

4 The SMASH model

56 4.1 Model overview

57 SMASH (Simulating Many Accelerated Strongly-interacting Hadrons) model,
58 created in 2018, is based on hadronic transport approach. This approach have
59 been successfully applied to describe the dynamical evolution of heavy ion col-
60 lisions since many years. The goal of model is to provide baseline calculations
61 with hadronic vacuum properties to identify signals of the phase transition to
62 the quark-gluon plasma. All information about the model can be read [8].

63 The main advantage of microscopic transport approach is that the full phase-
64 space information of all particles is available at all times. Model uses the most
65 well-established hadronic states from the Review of Particle Properties [9] with
66 their corresponding decays and cross sections.

67 It constitutes an effective solution of the relativistic Boltzmann equation
68 with binary interactions. Most interactions proceed via resonance excitation
69 and decay at lower energies or string excitation and fragmentation at higher
70 energies.

71 4.2 Event generating

72 For all calculations SMASH-1.6 has been used.

73 Was generated 10^6 of Au+Au collisions at energy $\sqrt{s_{NN}} = 11.5$ GeV with
74 time $t < 20 fm/c$ after collision and time step $\delta t = 1 fm/c$. The impact pa-
75 rameter is in range from 0 to 10 with "quadratic" distribution - use areal input
76 sampling (the probability of an input parameter range is proportional to the
77 area corresponding to that range $sP(b) = b * db$).

78 Potentials was off. Fermi motion was set frozen. Calculation Frame used
79 center of velocity.

5 Velocity and vorticity fields

80

5.1 Velocity weighting

81

82 To make the distribution of particles more uniform in coordinates and in mo-
 83 menta, a Gauss weighting was made. At fig. 1 the three plane projection of the
 84 cell velocity (1) for all particles with no weighting at time $t = 10\text{fm}/c$. This is
 85 projections from 3d plot, and they sum all slices (near less than 40). So we the
 86 values are more than 1. However at 1 slice this distribution looks like 1 right
 87 down figure. So velocity lowers to the center.

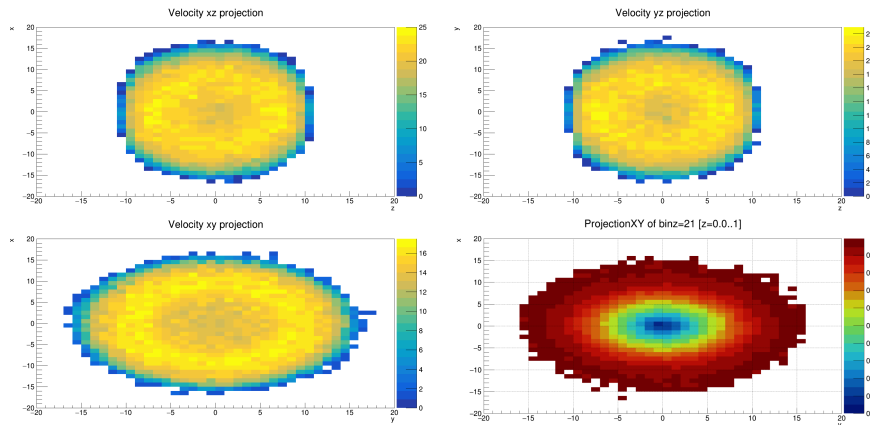


Figure 1: The three plane projection of not weighted velocity at $t=10\text{fm}/c$ and right bottom 1 slice XY projection, $z=0-1\text{ fm}/c$.

88

89 The same was made for weighted particles. As we can see at fig 2 weighted
 90 velocity is smoother. This means that it is less susceptible to random fluctua-
 91 tions. And when we will calculate the derivatives numerically, the values will
 be more even and accurate.

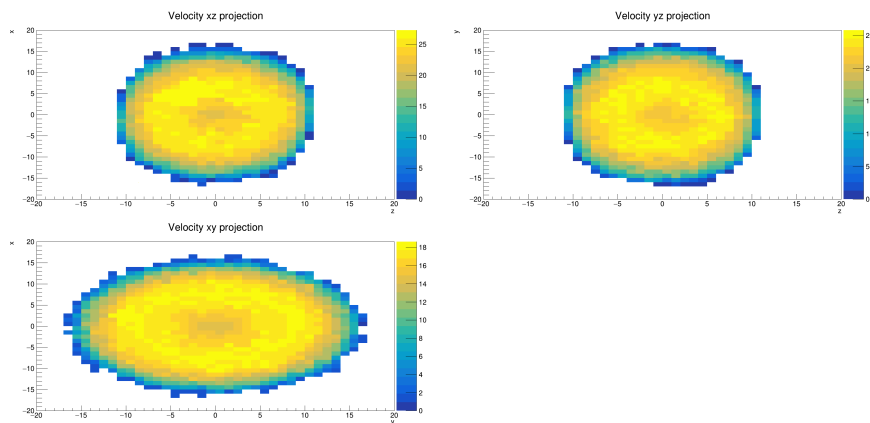


Figure 2: The 3 plane projections of weighted velocity at $t=10\text{fm}/c$

92 **5.2 Vorticity calculation**

93 The vorticity was calculated using discrete partial derivatives. We use numerical
 94 differentiation by three nodes, where possible, and differentiation by two nodes
 95 was used at the edges.

96 At the figure 3 is shown vorticity projection in reaction plane at y from 0
 97 to 1 fm/c. We can see the quadrupole-like structure. The upper figures show
 98 the vorticity values. While the bottom only it sign. It can be seen that in the
 99 center of the structure its value tends to 0. At the borders, since the derivative
 100 is calculated less accurately and, possibly, there are few particles, we observe
 101 strong fluctuations. The vorticity cells with values more than 0.1 were excluded,
 because they are observed only at the borders in a small number of cells.

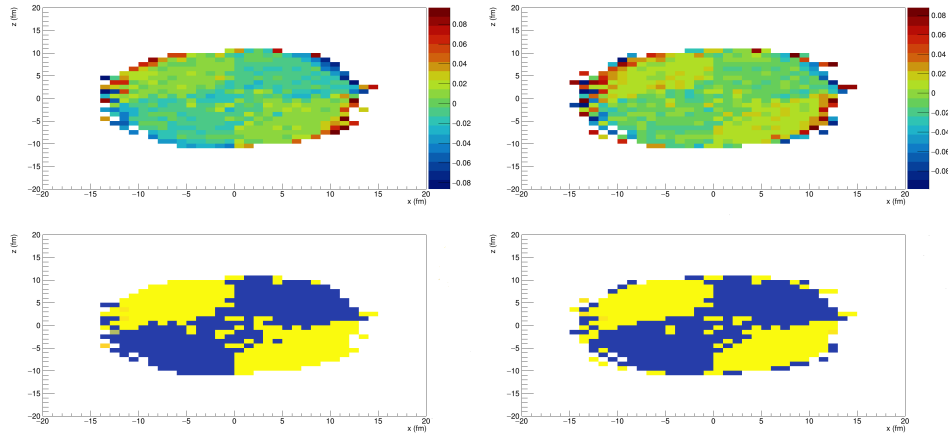


Figure 3: Vorticity projection in reaction plane. Used different methods of calculation velocity: Right (1), Left (2). Top is projection, bottom is sign: blue - negative, yellow - positive

102 The figure 4 contains all vorticities, but we can't see the quadrupole-like
 103 structure. And some big values near the border. That changes sign from cell to
 104 cell and must be taken more accurate.
 105

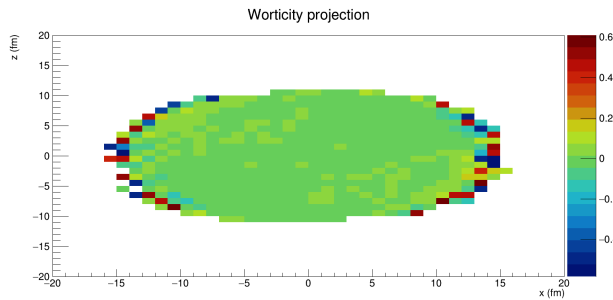


Figure 4: Vorticity projection in reaction plane. First method of finding velocity.

106 Than we made ratio for this two methods for all cells, and for cells with
 107 vorticity < 0.1 . As shown in figure 5 , for cells with any vorticity, the values
 108 diverge greatly, near 50%, while for cells with a value less than 0.1 they coincide
 109 within 2%. However This means that the methodology of calculating the vor-
 110 ticity strongly affects the boundaries and almost does not differ in the center.
 111 This effect is also possible due to a change in the method of calculating the
 112 derivative from three nodes to two at any coordinate.

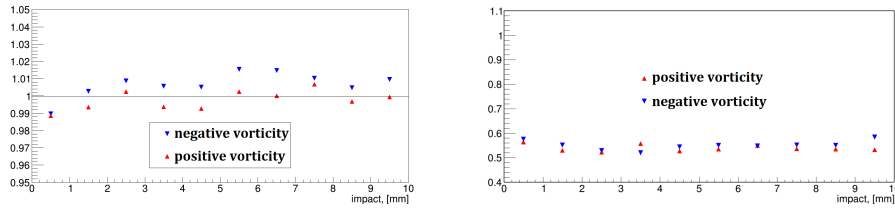


Figure 5: Vorticity ratio for 2 differen methods (2)/(1) with all cells (right) and only with vorticity less than 0.1 (left).

113 5.3 Helicity separation

114 For each impact parameter helicity was calculated for cells with positive and
 115 negative speeds separately. Because the sum helicity is near 0.

116 As shown at fig 6 helicity is not zero and changes the sign with the sign of
 117 the velocity y component calculated with (1).

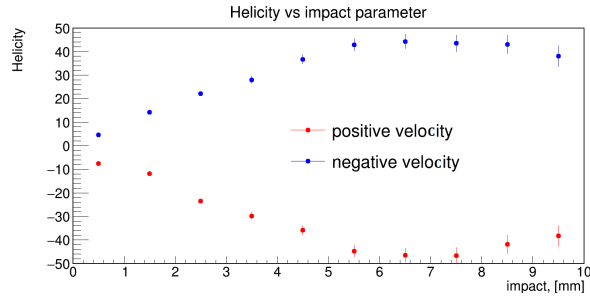


Figure 6: Helicity separation with positive and negative velocity

118 Also we compared the values obtained for helicity, depending on the method
 119 for determining the velocity. As it can be seen from the figure 7, the values
 120 obtained by method (1) are slightly larger than those obtained by the (2). With
 121 impact parameter < 1 mm the values are very different, since very central
 122 collisions occur.

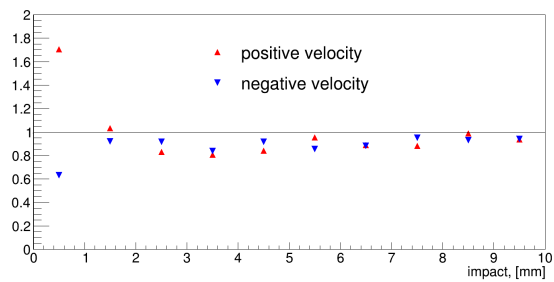


Figure 7: Helicity ratio for 2 different methods of calculating velocity.

123 **6 Conclusion**

124 At this analysis we calculated the following physical quantities within SMASH
125 model: velocity, vorticity and hydrodinamical helicity. All valies was calcu-
126 lated for all particles. Was used two different definitions for velocity, that has
127 some differences in final values. Also particle weighting makes distribution more
128 smooth, which leads to more accurate values of the derivative.

129 During the analysis were shown quadrupole-like structure of vorticity in reac-
130 tion plane and helicity sign changes with velocity, two methods works practically
131 the same for low vorticities, and has some differences with huge values.

132 **7 References**

133 **References**

- 134 [1] F. Becattini, F. Piccinini and J. Rizzo, Phys. Rev. C77,024906 (2008).
135 [2] L. P. Csernai, V. K. Magas, D. J. Wang, Phys. Rev. C87, 034906 (2013)
136 [3] L.P.Csernai, V.K.Magas, H.Stocker, and D.D.Strottman, Phys. Rev. C84,
137 024914 (2011)
138 [4] L.P. Csernai, D.D. Strottman and Cs. Anderlik, Phys.Rev. C85, 054901
139 (2012).
140 [5] S. Floerchinger and U.A. Wiedemann, JHEP 11, 100(2011); and J. Phys.
141 G 38, 124171 (2011)
142 [6] E. Gourgoulhon, EAS Publ. Ser.21(2006) 43
143 [7] M. Baznat, K. Gudima, A. Sorin and O. Teryaev, Phys. Rev. C **88** (2013)
144 no.6, 061901 doi:10.1103/PhysRevC.88.061901 [arXiv:1301.7003 [nucl-th]].
145 [8] J. Weil *et al.*, Phys. Rev. C **94** (2016) no.5, 054905
146 doi:10.1103/PhysRevC.94.054905 [arXiv:1606.06642 [nucl-th]].
147 [9] M. Tanabashi et al. (Particle Data Group) Phys. Rev. D 98, 030001 –
148 Published 17 August 2018